

clusters, i.e. to observe the very central regions (a few fractions of a parsec) with the maximum possible spatial resolution. To this aim, the VLT in its interferometric configuration is the *only* instrument capable of achieving the necessary resolution. If one could reach the nominal resolution of about 0.004 arcsec, one could really make an incredible step forward even compared to the best results one could possibly obtain from HST in its best configuration (~ 0.02 arcsec).

6. Conclusions

In conclusion, it is quite evident even from our schematic and incomplete review of globular cluster studies that the VLT will be an extremely important tool for yielding a better insight into most of the current hot problems. A fruitful complementarity exists between the results uniquely achievable from space (with HST, ISO, etc.) and those one can better obtain from the ground with the VLT and its many detectors. In this respect, it is important to note that (i) there are crucial observing programmes which require not only the use of the already planned VLT instruments (i.e. FORS, ISAAC, CONICA, UVES, and MFAS) but also of some instruments presently under study or just proposed like MIIS, NIR-MOS, FRISPI, and WFDVC; and (ii) several extremely important issues in the study of globular cluster problems can best be addressed in the IR wavelength range, and since neither HST nor ISO for various different reasons are able to carry out the necessary observations, IR instruments for the VLT (especially in the near and intermediate IR) should have a very high priority in the selection, construction and commissioning.

References

- Alcock C., *et al.* 1993, *Nature*, **365**, 621.
 Ambartsumian V.A. 1938, *Ann. Leningr. State Univ.* No. 22.
 Antonov V.A., 1962, *Vestn. Leningr. Gos. Univ.* 7, 135.
 Auburg E., *et al.* 1993, *Nature*, **365**, 623.
 Baily C.D. 1992, *ApJ*, **392**, 519.
 Bettwieser E., Sugimoto D. 1984, *MNRAS*, **208**, 439.
 Bolte M. 1992, *ApJ*, **376**, 514.
 Buonanno R., Corsi C.E., Fusi Pecci F. 1989, *A&A*, **216**, 80.
 Buonanno R., Corsi C.E., Fusi Pecci F., Richer H.B., Fahlman G.G. 1994, *AJ*, in press.
 Cacciari C., Clementini G., Fernley J.A. 1992, *ApJ*, **396**, 219.
 Chiosi C., Bertelli G., Bressan A. 1992, *ARA&A*, **30**, 235.
 Crocker D.A., Rood R.T. 1988, in *Globular Cluster Systems in Galaxies*, IAU Symp. No. 126, eds. J.E. Grindlay and A.G.D. Philip, Kluwer, Dordrecht, p. 509.
 Djorgowsky S.G., King I.R. 1986, *ApJL*, **305**, L61.
 Fahlman G.G., Richer H.B., Searle, L., Thompson I.B. 1989, *ApJ*, **343**, L49.
 Forte J.C., Mendez M., 1989, *ApJ*, **354**, 222.
 Frogel J.A., Elias J.H. 1988, *ApJ*, **324**, 823.
 Fusi Pecci F., Renzini A. 1976, *A&A*, **46**, 447.
 Fusi Pecci F., Renzini A. 1979 in *Astronomical Uses of the Space Telescope*, eds. F. Macchetto, F. Pacini, M. Tarengi (ESO), p. 181.
 Fusi Pecci F., Ferraro F.R., Corsi C.E., Cacciari C., Buonanno R. 1992, *AJ*, **104**, 1831.
 Fusi Pecci F., Ferraro F.R., Bellazzini M., Djorgovskij S.G., Piotto G., Buonanno R. 1993, *AJ*, **105**, 1145.
 Gillet F.C., deJong T., Neugebauer G., Rice W.L., Emerson J.P. 1988, *AJ*, **96**, 116.
 Goodman J. 1987, *ApJ*, **313**, 576.
 Gratton R.G., Sneden, C. 1989, *A&A*, **234**, 366.
 Helou, G. and Walker, D.W., 1986, *IRAS Small Scale Structure Catalog*, U.S. GPO, Washington D.C.
 Henon M. 1961, *Ann. d'Ap.*, **24**, 369.
 Hodge, P.W., 1983, *ApJ* **264**, 470.
 Käufel, H.U., Jouan, R., Lagage, P.O., Masse, P., Mestreau, P. and Tarrus, A., 1992, *The Messenger* **70**, 67.
 King I.R. 1966, *ApJ*, **71**, 64.
 Kraft R.P., *et al.* 1992, *AJ*, **104**, 645.
 Larson R.B., 1974, *MNRAS* **166**, 585.
 Le Fèvre O. 1994, in *Instruments for the ESO-VLT booklet*.
 Lynch D.K., Rossano G.S. 1990, *AJ*, **100**, 719.
 Majewski S.R. 1993, *ARA&A*, **31**, 575.
 McWilliam A., Rich R.M., 1994, preprint.
 Nemeč J. 1991, *Nature*, **352**, 286.
 Molaro P., Pasquini L., 1994, *A&A*, **281**, L77.
 Paresce F., De Marchi G., Romaniello M., 1994, preprint.
 Peterson R.C. 1983, *ApJ*, **275**, 737.
 Piotto G. 1993, in *Structure and Dynamics of Globular Clusters*, ASP Conf. Ser. 50, eds. S. Djorgovski & G. Meylan, p. 233.
 Pritchett C.J., Glaspey J.W. 1991, *ApJ*, **373**, 105.
 Reimers D., 1975, *Mem. Soc. R. Sci. Liège*, **6(8)**, 369.
 Renzini A. 1977, in *Advanced Stages of Stellar Evolution*, eds. P. Bouvier and A. Maeder, Geneva Obs., Geneva, p. 151.
 Renzini, A., 1977, in *Advanced Stellar Evolution*, P. Bouvier and A. Maeder eds., Saas-Fee, Geneva Obs., p. 149.
 Renzini A. 1985, *Astronomy Express*, **1**, 127.
 Renzini A., Fusi Pecci F. 1988, *ARA&A*, **26**, 199.
 Richer H.B., Fahlman G.G., Buonanno, R., Fusi Pecci F., Searle, L., Thompson I.B. 1991, *ApJ*, **381**, 147.
 Roberts M.S. 1988, in *Globular Cluster Systems in Galaxies*, IAU Symp. 126, J.E. Grindlay and A.G.D. Philip eds., Kluwer, Dordrecht, p.411.
 Sandage A.R., Cacciari, C. 1990, *ApJ*, **350**, 645.
 Sarajedini A., Demarque P. 1990, *ApJ*, **365**, 219.
 Schneps M.H., Ho P.T.P., Barrett A.H., Buxton R.B., Myers P.C. 1978, *ApJ*, **225**, 808.
 Seidl E., Demarque P., Weinberg D. 1987, *ApJS*, **63**, 917.
 Skinner C.J., Whitmore B. 1988, *MNRAS*, **231**, 169.
 Smith G.H. 1987, *PASP*, **99**, 67.
 Smith G.H., Wood, P.R., Faulkner, D.J., Wright, A.E. 1990, *ApJ*, **353**, 168.
 Spite M., Maillard J.P., Spite F. 1984, *A&A*, **141**, 56.
 Spitzer L. 1940, *MNRAS*, **100**, 396.
 Stryker L.L. 1993, *PASP*, **105**, 1081.
 Sweigart A.V., Mengel, J.G. 1979, *ApJ*, **229**, 624.
 Tinney C.G. 1994, in *Science with the VLT*, ESO-Garching.
 Vandenberg D.A., Bolte M., Stetson P.B. 1990, *AJ*, **100**, 445.
 Vandenberg D.A., Smith G.H. 1988, *PASP*, **100**, 314.
 Wampler E.J. 1994, in *Instruments for the ESO-VLT booklet*
 Zinn R.J. 1986, in *Stellar Populations*, Norman C.A., Renzini A. and Tosi M., eds., Cambridge University Press, Cambridge, p. 73.

Scientific Capabilities of the VLT Adaptive Optics System

B. THÉODORE¹, P. PETITJEAN² and N. HUBIN¹

¹ESO-Garching; ²Institut d'Astrophysique de Paris, France

1. Introduction

The theoretical angular resolution power of a telescope of diameter D

is limited by diffraction and is proportional to λ/D . However, atmospheric turbulence severely restricts the capabilities of astronomical telescopes. What-

ever the aperture diameter, the resolving power of the telescope is limited by the seeing angle and so the image of a point source is spread most often

over more than 0.7 arcsec in the visible. A radical way to achieve the diffraction limit is to put the telescope above the atmosphere. Though this allows high-quality imaging as demonstrated by the recent breakthrough of HST, this is rather involved and expensive. Different techniques are used to approach diffraction-limited imaging using ground-based systems, like speckle, long-baseline interferometry or post-observation deconvolution. However, adaptive optics is the simplest way for observers to overcome in real time the perturbations induced by the atmosphere on ground-based telescopes without any further image processing (Merkle 1988).

This motivates the growing interest for adaptive optics systems and explains why several prototypes are being built all over the world. Up to now, the only system allowing nearly full correction of the atmospheric perturbation and offered to visiting astronomers is the COME-ON+ system at the 3.6-m telescope of ESO.

This system has obvious limitations: it requires for instance relatively bright stars ($m_V < 13$) for use as a reference by the wavefront sensor. The relatively small diameter of the telescope restricts the possibility of this instrument. But the experience acquired by using it will greatly help designing the system to be installed at the VLT. An obvious task is to assess the scientific capabilities of such a system. After describing the effect of atmospheric turbulence on the images and the way they can be compensated we will present results of calculations of the fraction of the observable sky using this technique.

2. Effect of Atmospheric Turbulence on Astronomical Images

The refractive index along a path through the atmosphere exhibits spatial and temporal variations due to atmospheric inhomogeneities. As a result, an initial plane-parallel wavefront arrives distorted at the telescope. The variations of the phase in a reference plane may be described by the *phase structure function* D_ϕ , which is the variance of the phase variations between two points of the plane. This quantity is a function of the atmospheric characteristics and is not known in general. Assuming, however, that atmospheric turbulence obeys Kolmogorov statistics, it can be shown that D_ϕ is proportional to the five-third power of the distance r between two points.

$$D_\phi(r) = 6.88(r/r_0)^{5/3} \quad (1)$$

where r_0 is the characteristic coherence length known as *Fried parameter*. The latter is related to the seeing angle $\theta_s = \lambda/r_0$ and increases with the

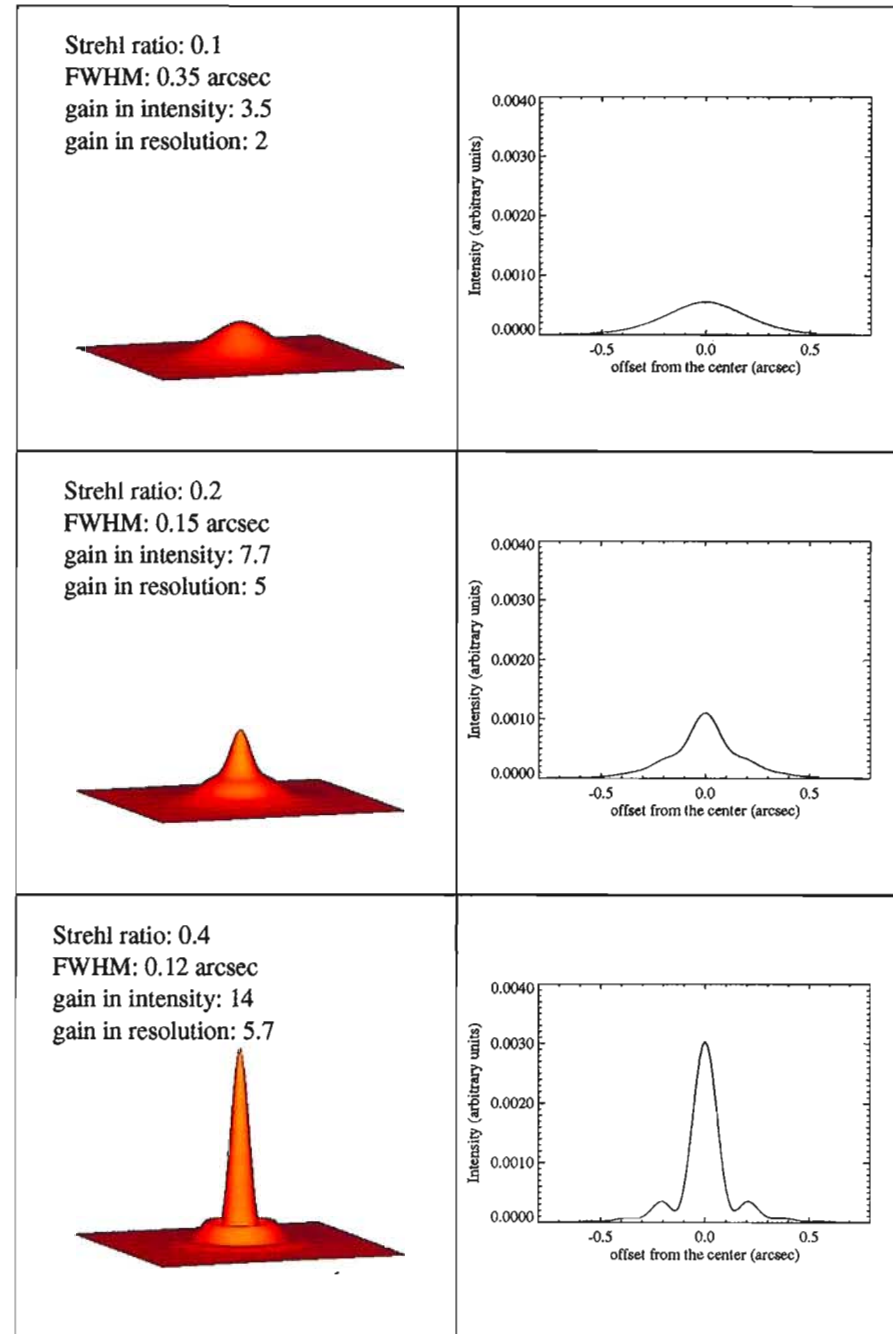


Figure 1: Shape of the image after compensation. **Top:** moderate correction (Strehl ratio = 0.1): the image is Gaussian, but the compensation leads to a gain of a factor of 3.5 in intensity and 2 in resolution compared to the uncompensated image. **Middle:** Strehl ratio = 0.2: a coherent core appears, surrounded by a halo. The image is much sharper compared to the uncompensated one. **Bottom:** Strehl ratio = 0.4: the image is diffraction-limited and surrounded by a faint halo.

wavelength as $\lambda^{6/5}$. It is also the diameter of an aperture through which, for given atmospheric and zenith angle conditions, nearly diffraction-limited images can be obtained; the images appearing to change position as the atmosphere evolves with time. This means that phase variations on such a distance are small enough so that the image profile is not altered. This means also that this is the diameter of the aperture through which

a unique phase error (the motion of the image in the field of view) may be measured and compensated by actuating a single mirror.

Overcoming the distortions induced by atmospheric turbulence on an incoming wavefront requires thus the sampling of the wavefront through areas of diameter r_0 , or less, in a reference plane. This is the role of the wavefront sensor as it will be described later. For a large tele-

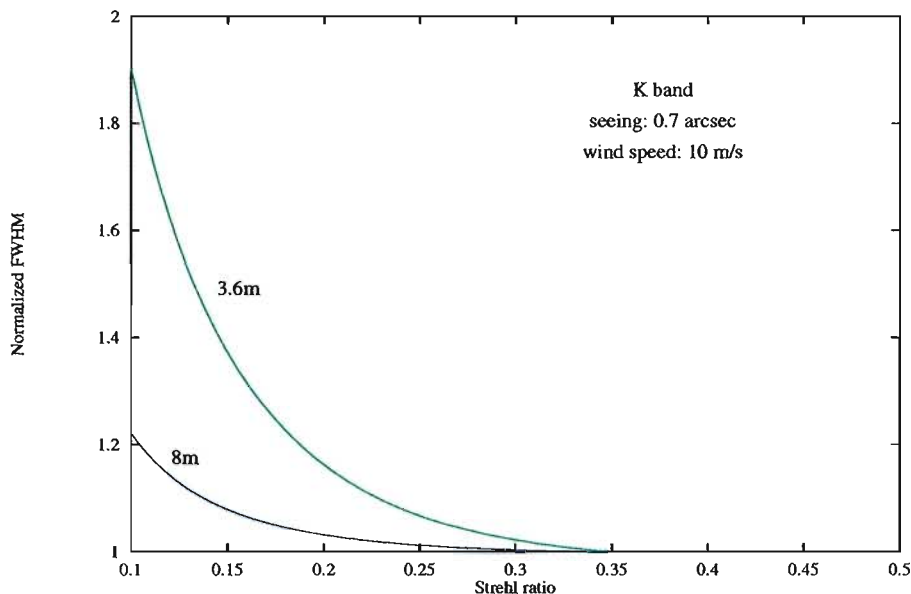


Figure 2: FWHM of the image (in units of the FWHM of the diffraction-limited image) as a function of the Strehl ratio.

scope $(D/r_0)^2$ is thus the optimal number of actuators to be used to shape the deformable mirror of the adaptive optics system. While the average value of r_0 at La Silla is 12 cm at $0.5 \mu\text{m}$, it is 71 cm at $2.2 \mu\text{m}$. It is thus easier to build a system to compensate for the turbulence in the near-infrared since, for a given telescope, one needs fewer actuators in the infrared than in the visible. However, since the deformations of the wavefront do not depend on the wavelength, the wavefront sensing is performed in the visible, allowing thus the use of fainter objects as references, due to the higher performances of optical detectors.

3. Compensation of Atmospheric Turbulence

Once the phase variations on the telescope pupil are known, it is mathematically convenient to expand them on a base of orthogonal polynomials. The Zernike polynomials Z_i are often used, because they are representative of the classical optical aberrations (Noll 1976)¹. The first order is the piston and represents a translation of the wavefront along the optical axis; thus it has no effect on the image shape. The second and third orders are the tilt in x and y directions which cause the image to move in the field of view, the fourth order is the defocus which causes the rays to cross the optical axis out of the theoretical focus

of the mirror, the eleventh order is the spherical aberration, etc...

The wavefront distortions may now be written:

$$\phi = \sum a_i Z_i \quad (2)$$

Thus, in order to compensate for the wavefront aberrations, one must correct the wavefront in order to set the coefficients a_i of the expansion to zero or, at least, to minimize them.

It is interesting to assess the influence of a perfect compensation of the first N Zernike orders ($a_{i(i=1, \dots, N)} = 0$). It is indeed possible in this case and under the usual hypothesis of a Kolmogorov turbulence to derive the residual variance of the phase on a reference plane:

$$\sigma^2 = 0.2944N^{-0.866} \left(\frac{D}{r_0}\right)^{5/3} \quad (3)$$

The residual is of course a decreasing function of the number of corrected modes N , since the more numerous the corrected orders the better the correction. It is also an increasing function of (D/r_0) . Indeed for the same atmospheric conditions and at the same wavelength, the variation of the phase is larger on a larger distance (or here aperture) and, for the same aperture, it is larger for worse seeing (thus smaller r_0).

The residual phase variance as a way for evaluating the image quality is rather vague. A more relevant parameter is the Strehl ratio, which is the ratio of the maximum intensity of a point source image to the maximum intensity of the diffraction-limited image through the same telescope. The larger the Strehl ratio, the closer the image from the ideal case of a diffraction-limited image. Though the Strehl ratio is defined and computed from the intensity in the image, it is also a

good indicator of the image structure and sharpness. This is illustrated in Figure 1 where image profiles are drawn for different Strehl ratios. For small values, the image is almost Gaussian in profile with a width equal to the seeing angle. As the Strehl ratio increases (i.e. as the correction becomes better), the image exhibits two components: a diffraction-limited core surrounded by a halo, the importance of the latter decreasing as the Strehl ratio rises (more and more light is concentrated in the core). This is illustrated in Figure 2, which shows the normalized FWHM as a function of the Strehl ratio: it decreases very sharply for small Strehl ratios until the sharp core is dominant. Then, the image is diffraction-limited in terms of resolution and increasing the Strehl ratio only increases the intensity in the core.

For the VLT, a Strehl ratio of 0.1 corresponds to a gain in resolution and in the maximum intensity of the image of a factor of 3.2 and of a factor of 5.6 respectively. We will consider in the following, somewhat arbitrarily, that this value of the Strehl ratio is the minimum acceptable correction for any observations using adaptive optics.

4. Adaptive Optics Systems

Adaptive optics systems have been extensively described elsewhere (e.g. Rigaut 1993). We briefly review the components of the system through the constraints they put on astronomical imaging.

Figure 3 recalls the basic arrangement of an adaptive optics system and the main steps of the compensating process: the wavefront distortions are analysed by the wavefront sensor, the phase is reconstructed and the optical train of the telescope is adapted in real time. This cycle must be carried out rapidly enough so that the atmosphere has not changed between the evaluation of the phase errors and the deformation of the mirror.

As alluded to above, the wavefront sensing consists in estimating the phase variations on a reference plane. This is done by sampling the wavefront on a pupil plane by an array of lenses, each of them forming an image on a detector. Ideally (in case there are no aberrations), the image produced by each lens is aligned with its optical axis. Otherwise, the position of the image gives an estimate of the averaged slope of the wavefront over the lenslet area. Thus, the correction of the wavefront will be optimal if the wavefront can be considered as planar over each lenslet. This is the case, as a first approximation, if each lenslet corresponds to a sub-aperture of diameter r_0 . Yet, since the Fried parameter is a function of the wavelength and in ad-

¹ Several bases may be used for the phase expansion (Rigaut, 1993), such as Karhunen-Loève functions which are more representative of the atmospheric turbulence, or the eigenmodes of the deformable mirror. We only address here the Zernike decomposition, because it is conceptually simpler.

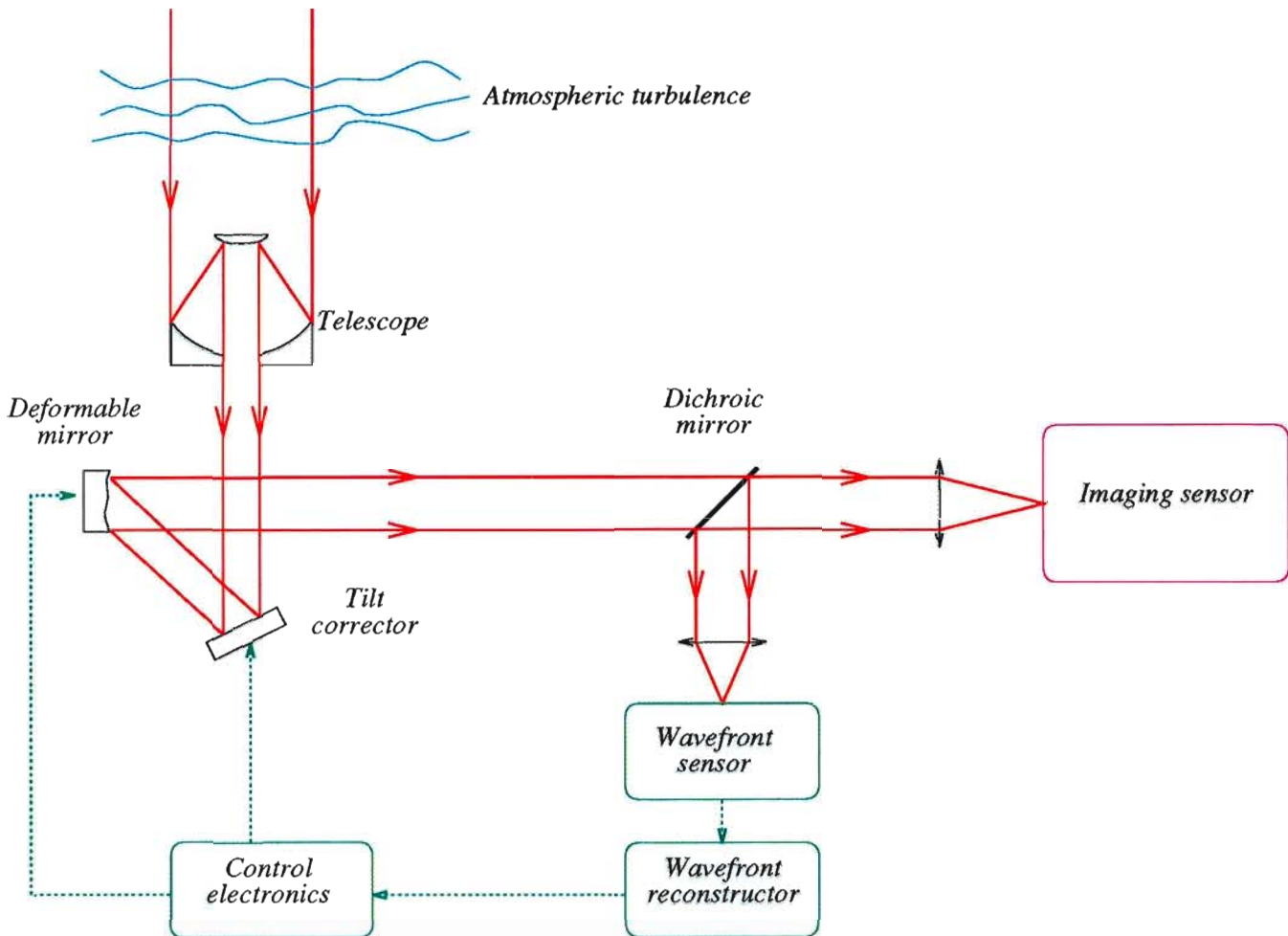


Figure 3: Arrangement of an adaptive optics system, showing the main steps of the compensation process: detection of the wavefront, reconstruction of the phase, adaption of the optical train. For the latter step two distinct mirrors are used in the COME-ON+ system.

dition exhibits a high temporal variability, the sampling cannot always be optimal since the number (and thus the diameter) of each sub-aperture is fixed by the design of the system².

A second constraint is that the time between two successive corrections must be shorter than the coherence time of the turbulence. The latter varies like r_0 as a function of the wavelength and is about 10 milliseconds at $2.2 \mu\text{m}$. Consequently the integration time on the reference object must be shorter than this, which, for a reasonable S/N ratio, requires the correction to be done using a bright enough object (either the object itself or a reference star). If the S/N ratio is not large enough, the position of the image of the reference star through the sub-apertures is not well determined and the correction is bad. Thus the ability of the system to compensate for the wavefront distortions depends on the magnitude of the reference star. This is illustrated in Figure 4 which shows the expected

Strehl ratio when using the current system COME-ON+ and the future system for the VLT as a function of the magnitude of the reference star for various wave-

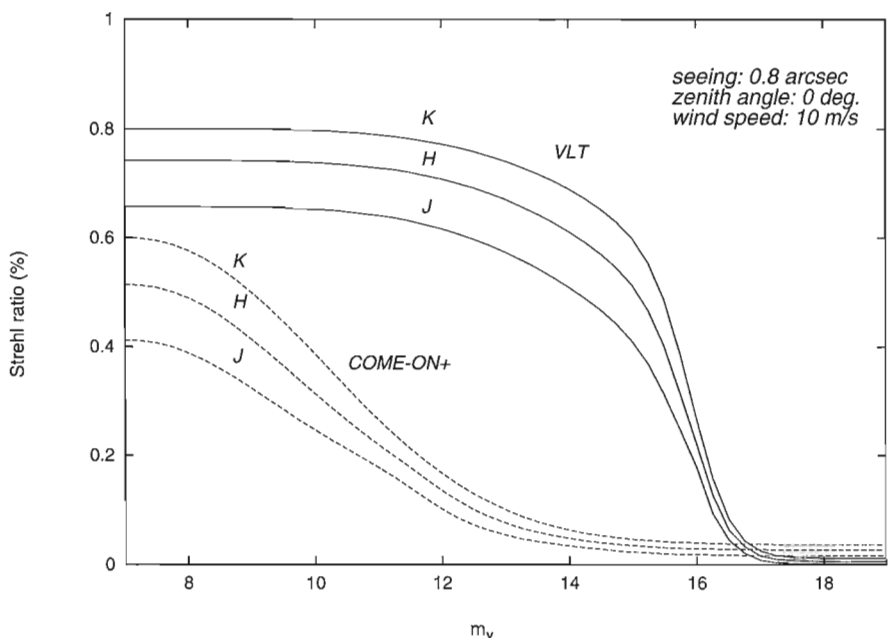


Figure 4: The correction is a function of the magnitude of the reference object. We show here the Strehl ratio achieved in J-, H- and K-bands versus the visible magnitude m_v of the reference star.

²Note that it is nevertheless possible to alleviate the problem of a super-sampling of the wavefront using, for example, modal control optimization.

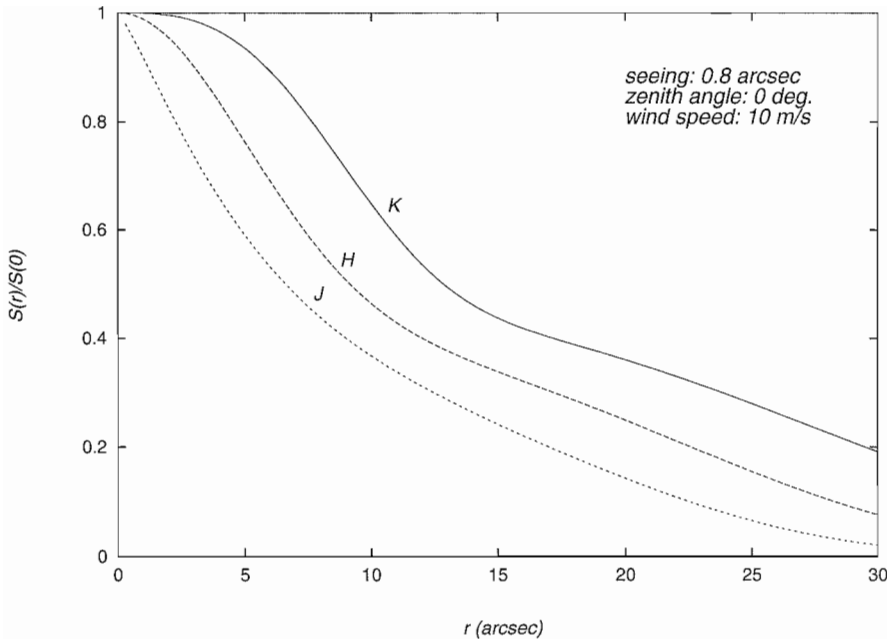


Figure 5: Using a reference star distinct from the observed object leads to a degradation of the correction (isoplanatic effect). The ratio of the Strehl ratio achieved on an object to the one achieved on a reference star is plotted versus the separation r between the object and the star.

bands and for a seeing of 0.8 arcsec (average value at Paranal). These curves were generated from experimental values for COME-ON+ and from a model for the VLT system (Hubin *et al.* 1993). For both systems there is a plateau up to a given magnitude (16 for the VLT⁺ and 13 for COME-ON+). Indeed, there is a minimum S/N ratio (obtained using a reference star of magnitude m_{lim}) above which the position of the images of the reference star given by each lenslet are well defined, yielding the correction to be optimal for all S/N ratios larger than this value (thus all reference stars with magnitude smaller than m_{lim}). At larger magnitudes, a rapid drop is observed because the signal of the reference star is too faint for the phase to be properly reconstructed. It may be noted also that even if the star is bright, the Strehl is not equal to one since the correction cannot be perfect due to the *de facto* discontinued sampling.

A third constraint on astronomical observation using adaptive optics is that quite a number of the objects of astronomical interest are not bright enough to achieve a proper correction ($m > m_{lim}$). In such a case a reference star is needed in the vicinity of the observed object. But since the atmosphere is not exactly the same along both lines of sight, towards the object and the reference star, the correction on the object is only partial even if the correction on the reference star is very good. This effect is called the isoplanatic angle limitation and is illustrated in Figure 5 where the ratio of the Strehl ratio achieved on the object to the one achieved on the reference star is plotted

as a function of the separation between both objects and for various wavebands. It is a rapidly decreasing function of the separation: for instance, in the K-band, if the reference star lies at 12 arcsec from the astronomical object, the Strehl ratio achieved on the latter is half the one achieved on the former.

Thus, the quality of the corrected image is essentially a function of two parameters: the magnitude of the reference star and its separation from the ob-

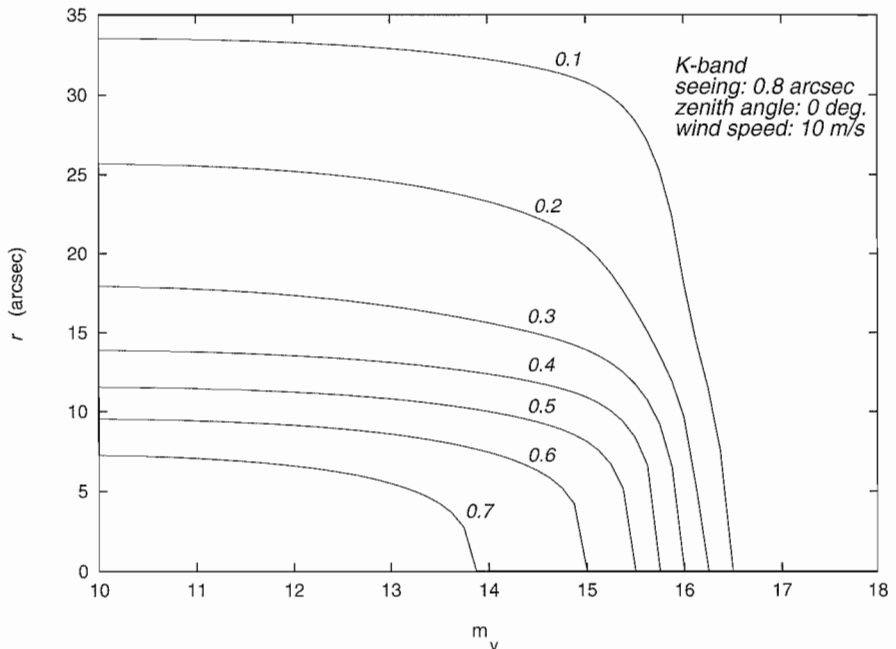


Figure 6: Strehl ratio achieved in K-band with the VLT system plotted as a function of the magnitude m_v of the reference star and of the separation r between the observed object and the reference star.

served object. This is illustrated in Figure 6 which gives the Strehl ratio which will be achieved with the VLT system in the K-band as a function of these two parameters, the magnitude m_v and separation r . As an example, if the correction is done using a star of magnitude 15, the Strehl ratio at 30 arcsec of the object is 0.1 in the K-band for 0.8 arcsec seeing conditions and a 10 ms^{-1} averaged wind speed. On the star itself, a Strehl ratio of 0.6 could be expected.

5. Potential Observations

The necessity to find a bright reference star as close as possible (and in any case within one arcmin) from the observed object is a severe constraint and limits the possibility of the system in terms of sky coverage. Indeed, the probability of finding such a star is rather small. We have quantified this probability using two approaches: the first one is to compute the fraction of the sky which may be observed at a given level of correction. The second one is to evaluate the expected distribution of improvement level by cross-correlating catalogues of potentially interesting objects with catalogues of bright stars.

5.1 Sky coverage

Given the characteristic of an adaptive optics system, it is possible to compute the area of the sky surrounding any bright star in which the system will allow a given level of correction when using the star

as reference object. For a given system, this area depends on the magnitude of the star and the level of correction aimed at. Integrating over the whole sky gives the fraction of the sky that is possible to observe in those conditions:

$$\xi(S) = \int_{m_{min}}^{m_{max}} n(m) \pi r^2(m, S) dm$$

where m_{min} is the magnitude of the brightest reference star considered, m_{max} is the magnitude of the faintest star possibly used for correction by the system, $r(m, S)$ is the radius where the Strehl ratio is S and $n(m)$ is the density of stars of magnitude m .

The density of stars has been estimated from the Guide Star Catalogue (hereafter GSC). It is however complete up to magnitude 14.5 only and we used the Galactic models by Bahcall and Soneira (1980) for fainter stars. Actually, the distributions from the GSC and the models are in very good agreement for magnitudes smaller than 14.

The sky coverage as a function of m_{max} for regions of the sky just above the galactic plane and for various Strehl ratios is shown in Figure 7a for COME-ON+ and 7b for the VLT system. It is a steep function of the magnitude till it reaches a plateau. The latter is mainly due to the sharp drop of the performances of the system for faint reference stars (see Figure 4).

The possibilities of COME-ON+ appear to be rather restricted since even for a Strehl ratio of 0.1, the sky coverage is less than 0.35%. For the VLT, the observable fraction of the sky can reach 17% for a Strehl ratio of 0.1 with the magnitude limit $m_{lim} = 16$ for the reference star. With a magnitude limit of 17, more than a quarter of the sky could be observed with a Strehl ratio of 0.1 in the K-band for 0.8 arcsec seeing conditions and a wind speed of 10 ms^{-1} . On the other hand, about 2% of the sky is observable with a Strehl ratio of 0.4.

As shown above, both the Strehl ratio achieved on the reference star and the isoplanatic angle are wavelength dependent. These quantities vary in a similar way, leading the Strehl ratio to be larger at higher wavelengths even for large separations. However, the gain in resolution is restrained by the increase with wavelength of the FWHM of the diffraction-limited image with the wavelength. Thus, the K-band ($2.2 \mu\text{m}$) seems to be currently the best compromise for adaptive optics observations.

5.2 Specific objects

In the previous paragraph the approach was purely statistical with no consideration of the presence or absence of interesting objects in the surveyed area.

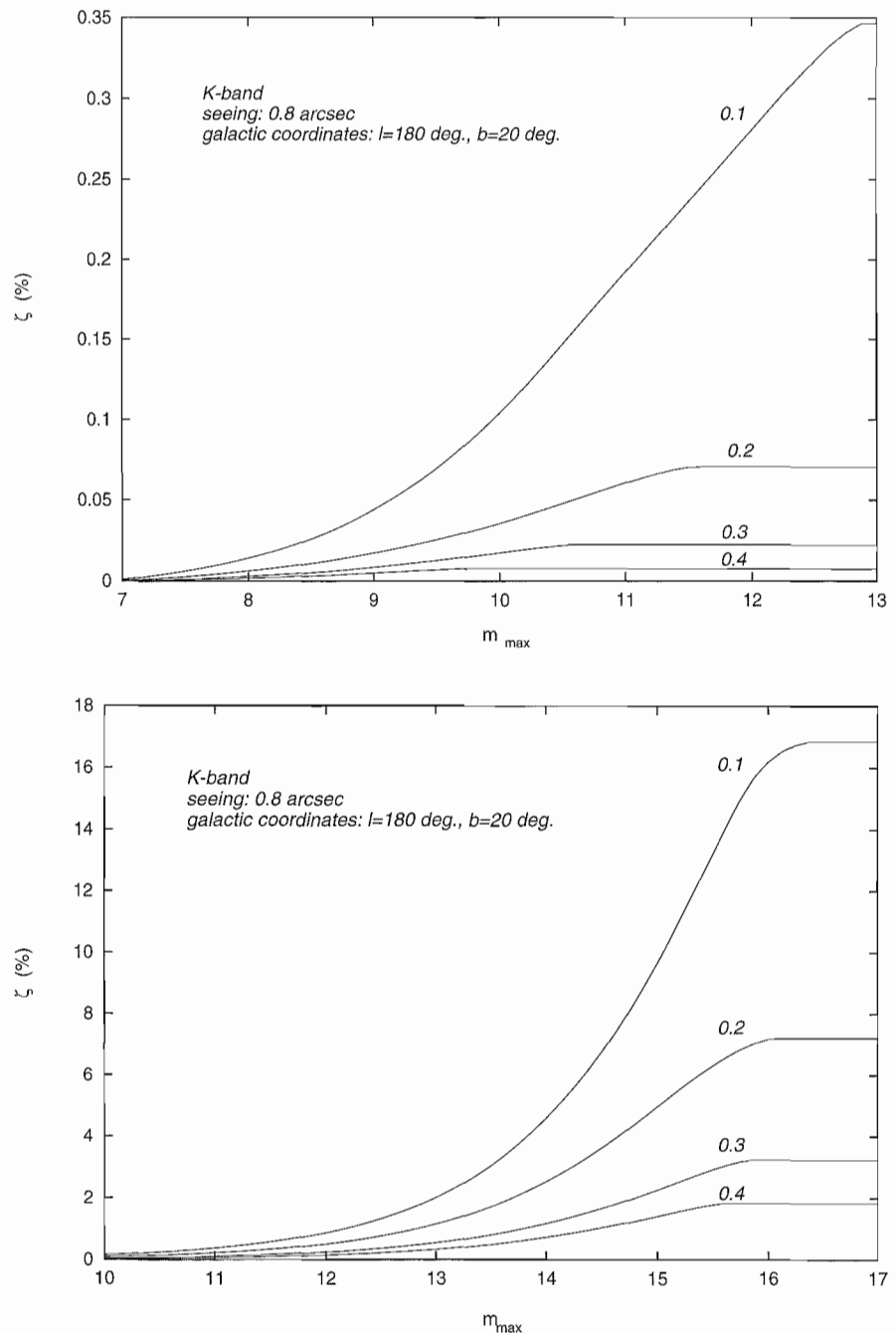


Figure 7: Sky coverage versus the largest possible magnitude of the star used as reference m_{max} for several Strehl ratios (0.1, 0.2, 0.3, 0.4) achieved with COME-ON+ (top) and the VLT (bottom) systems.

A few projects will use this approach such as random search for very high redshift field galaxies. However, this is not the usual way of investigation: one aims indeed at observing a specific object. In this case, and until laser guide stars become available, the observation depends on the presence of a bright star in the vicinity of the target and this defines the correction one might expect during the observation.

Following this line one may ask for the probability to achieve a given correction when observing a sample of predefined scientific targets. This was our second

approach to assess the potential of the system. To do so a catalogue of targets is cross-correlated with a bright star catalogue. Given the coordinates of the objects, the star catalogue is searched for the star that would give the best correction. A quite similar approach has been followed by Bonaccini *et al.* (1993) in the context of the Italian Galileo project. In their study, however, the image quality does not appear clearly. As an example, we use as a list of possible targets the IRAS point source catalogue, which contains about 250,000 objects, and the HST Guide Star Catalogue for the ref-

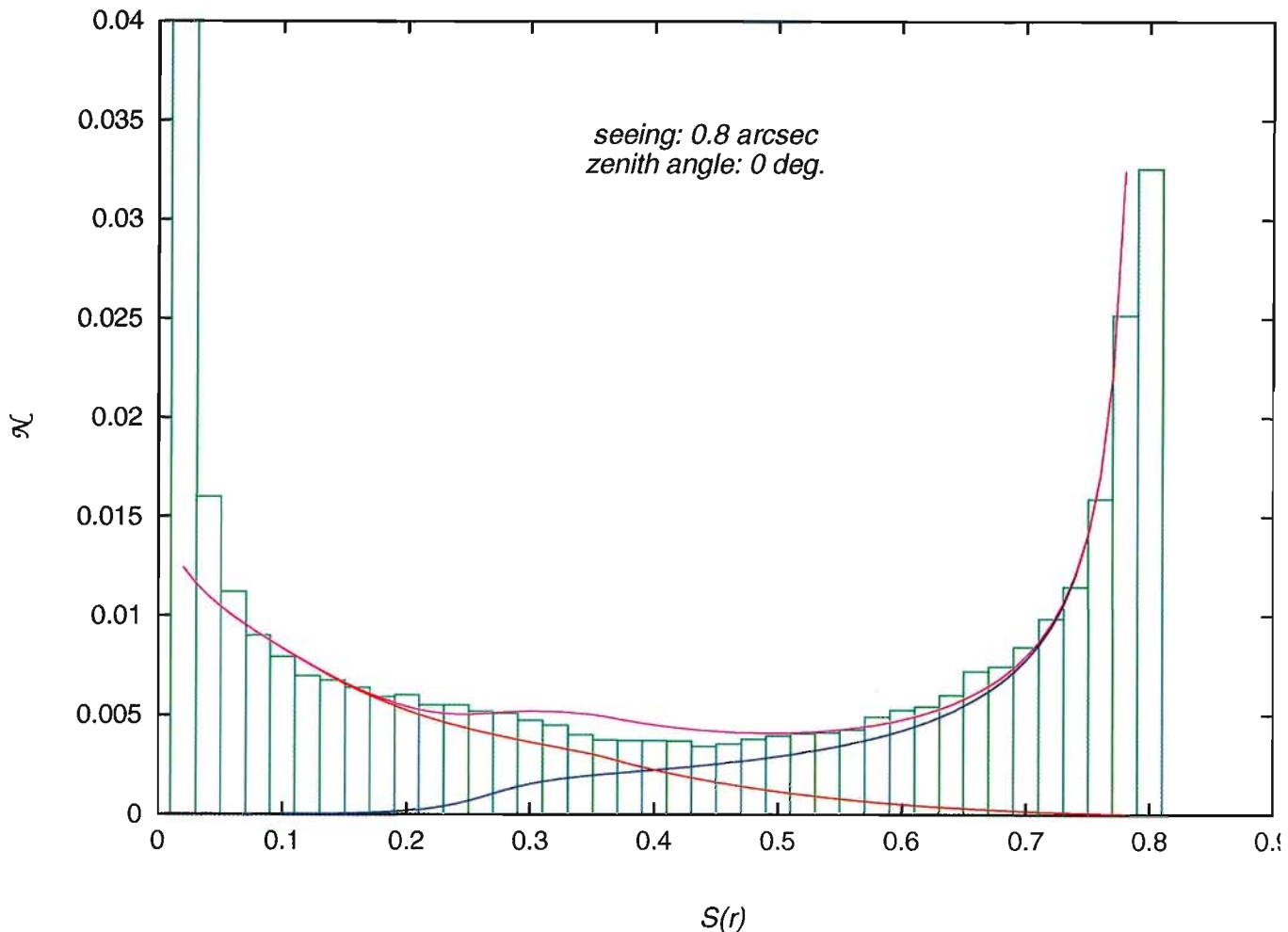


Figure 8: Percentage of IRAS objects observable with a Strehl ratio within the range $S - 0.01$, $S + 0.01$, obtained from cross-correlation between the IRAS point source catalogue and the Guide Star Catalogue. Overplotted is a model (in magenta), made up with two contributions. The green curve corresponds to observations using a nearby bright star as the reference. The blue curve corresponds to objects bright enough to be used as the reference source.

reference star catalogue. For each object, a star was searched in the GSC within 1 arcmin and, if present, the Strehl ratio was computed using the characteristics of the VLT adaptive optics system shown in Figures 3 and 4. About 89,000 objects were found to have a star lying within 1 arcmin, which holds for about one third of the catalogue. Figure 8 shows the distribution of Strehl ratios we obtained. Along the y-axis is plotted the fraction of IRAS objects (compared to the whole catalogue) observable at a given correction level. The fraction of observable objects strongly increases at both ends of the diagram. At the small Strehl ratio end, this is because the probability of finding a star in the vicinity of a given object increases as the square of the separation, and thus the probability for a small Strehl ratio increases. At the large Strehl ratio end, there is a large contribution of objects which are present in both GSC and IRAS catalogues. These objects can be used themselves as the reference source and the achieved Strehl ratio is large. Since most of the objects in the GSC have magnitudes smaller than 15, the correspond-

ing Strehl ratio should be most of the time very close to 0.8 and the distribution should be strongly peaked around this value. It can be seen however that the distribution is broad because, due to imprecision in the astrometry, the coordinates of a number of these objects differ in both catalogues.

These two contributions have been modeled. Assuming that stars are randomly distributed in the sky, the distribution of the Strehl ratios possibly achieved at given points of the sky can be computed and is shown as a red curve in Figure 8. To do this, we used the Bahcall and Soneira (1980) models. The second contribution has been computed assuming that the differences in the position of an object in IRAS and GSC obeys Gaussian statistics, with a dispersion chosen to fit the data best. This is the blue curve on Figure 8. The final distribution (in magenta on the plot) is the sum of these two contributions, and one can see that it fits reasonably well the distribution we obtained from the cross-correlation, some of the discrepancies resulting from imperfections of the star catalogue.

One of the most important limiting factors is the magnitude limit of the corrective system. This is particularly true for COME-ON+ which has a limiting magnitude of about 13 for averaged meteorological conditions, that is 0.8 arcsec seeing and 10 ms^{-1} wind speed. For the VLT system it is expected to be somewhat larger in the same conditions. It is of importance to define what would be the optimal magnitude limit. This is particularly important for extragalactic studies and can be investigated, for example, by looking at the number of QSOs as possible targets of such a system. QSOs are indeed promising reference sources since a number of extragalactic projects could use them (morphology of galaxies in clusters, absorption-line systems, host galaxies, etc.). In Figure 9a the distribution of quasars found in the Hewitt & Burbidge catalogue (Hewitt & Burbidge 1993) is plotted as a function of the redshift and the magnitude. One can see the rapid increase, whatever the redshift, of the number of quasars beyond the magnitude 16–17, that is just beyond the foreseen magnitude limit of the VLT adaptive

optics system. This is more striking in Figure 9b where the number of quasars brighter than a given magnitude is plotted, still from the Hewitt & Burbidge catalogue. While there are about 200 quasars brighter than magnitude 16, there are about 600 QSOs brighter than magnitude 17. Thus improving the capabilities of the system by one magnitude could lead to an increase by a factor of 3 in the number of observable QSOs. To achieve this, the integration time of the wavefront sensor might be increased, to the detriment of the quality of the correction, since it results in a decrease of the bandwidth of the system. To achieve a Strehl ratio of 0.1 within 15 arcsec around all QSOs brighter than magnitude 17 would be of great interest.

6. Conclusion

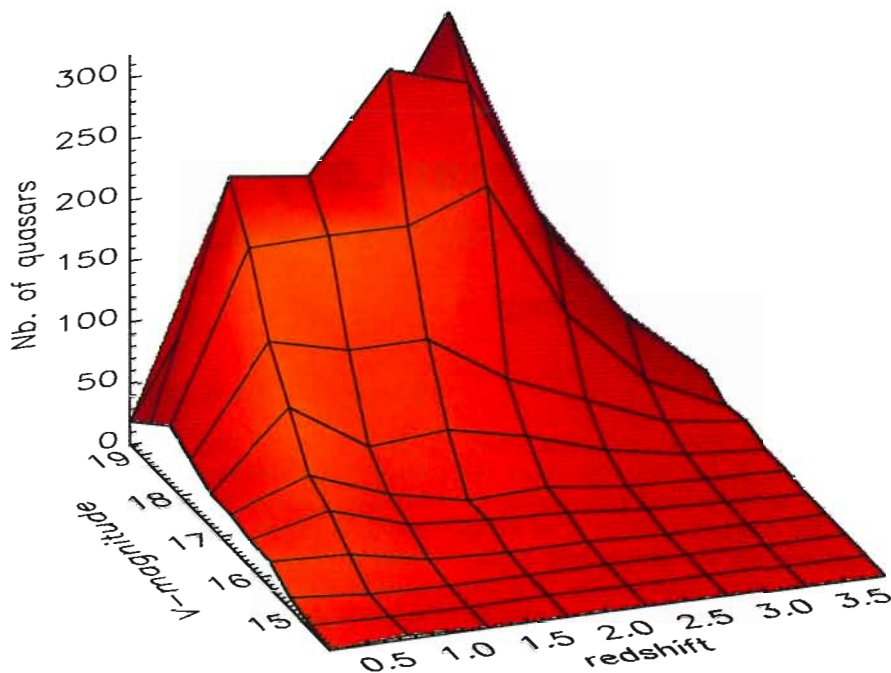
Adaptive optics is a promising technique to overcome the wavefront deformations induced by the atmospheric turbulence and to produce diffraction-limited quality images with ground-based telescopes. The rapid drop in quality of the correction with the distance to the reference star severely limits the fraction of the sky that is observable. This implies that the sky coverage of any adaptive optics system at a given wavelength strongly depends on the magnitude limit for the reference star. The latter should be larger than 17 so that about a quarter of the sky can be observed. This magnitude limit is also required if a copious number of QSOs (the most obvious extragalactic targets) shall become observable. The use of laser guide stars should resolve most of the above limitations (Rigaut and Gendron 1992).

To find a reference star near any potential target, a catalogue of such stars must be made available. It should be complete up to the magnitude limit of the system. At the moment the Guide Star Catalogue is complete down to magnitude 14.5.

It is clear that it is possible to build adaptive optics systems with large potentialities providing that they are able to improve the image quality in a large enough fraction of the sky. Moreover, we may expect exciting results using adaptive optics to perform very high spatial resolution spectroscopy of extended objects.

Acknowledgements

We would like to thank M.M. De Robertis for fruitful discussions. The cross-correlation of catalogues made use of the ESO/ST-ECF Archive Facility operated jointly by the European Southern Observatory and the European Space Agency.



Number of quasars brighter than a magnitude m

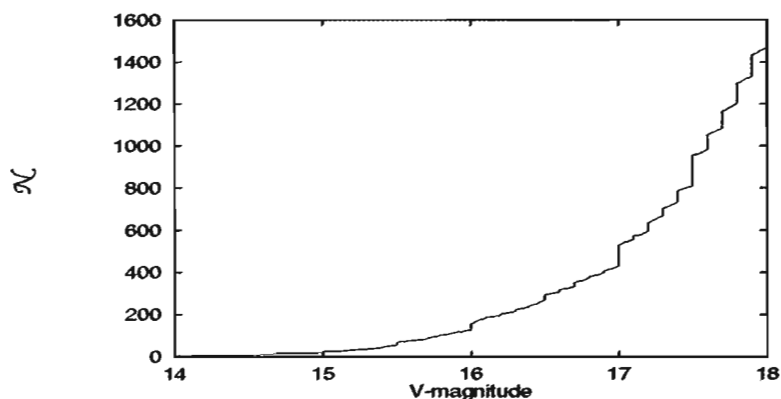


Figure 9: **Top:** Distribution of quasars in the Hewitt and Burbidge catalogue as a function of redshift and magnitude. Note the rapid increase of the number of quasars beyond the magnitude 16–17. **Bottom:** cumulative number of quasars brighter than a given magnitude as a function of the magnitude.

References

- Bahcall J., Soneira S., 1980, *ApJS* **44**, 73.
- Bonaccini D., Morbidelli R., Ranfagni P. 1993, Internal report of Torino Observatory n° 27.
- Hewitt A., Burbidge G., 1993, *ApJS* **87**, 451.
- Hubin N., Safa F., Stoffer R., in proc. of the ESO conf. on "Active and Adaptive Optics", Garching, 2–5 August 1993.
- Hubin N., Théodore B., Petitjean P., Delabre B., in proc. of the SPIE conf. on "Astronomical Telescopes and Instrumentation for the 21st Century", Kona, 13–18 March 1994.
- Merkle F., 1988, *The Messenger* **52**, 5.
- Noll R.J., 1976, *J. Opt. Soc. Am.* **66**, 207.
- Rigaut F., 1993, PhD Thesis dissertation, Univ. Paris 7.
- Rigaut F., Gendron E., 1992, *A&A* **261**, 677.